Journal of Applied Pharmaceutical Science Vol. 13(03), pp 044-052, March, 2023
Available online at http://www.japsonline.com
DOI: 10.7324/JAPS.2023.90862
ISSN 2231-3354

Prosochit®-based nanoparticulate system of insulin for oral delivery: design, formulation and characterization

Emmanuel O. Olorunsola[1*], Koofreh G. Davies[2], Koton P. Ibiang[1], Patience C. Esukpa[1], Ezinne G. Uwaechi[1], Fakhrul Ahsan[3]

[1]Department of Pharmaceutics and Pharmaceutical Technology, University of Uyo, Uyo - Akwa Ibom State, Nigeria.
[2]Department of Human Physiology, University of Uyo, Uyo - Akwa Ibom State, Nigeria.
[3]Department of Pharmaceutical and Biomedical Sciences, California Northstate University, Elk Grove California, United States.

ARTICLE INFO

Received on: 28/07/2022
Accepted on: 26/12/2022
Available Online: 04/03/2023

Key words:
Insulin, nanoparticles, oral delivery, Prosochit®.

ABSTRACT

Oral delivery is a promising mechanism for improving adherence to insulin therapy in diabetes management. This work was aimed at preparing and characterizing Prosochit®-based nanoparticles of insulin for oral administration. Insulin-loaded nanoparticles were formulated by the water-in-oil-in-water double emulsion-freeze drying method using three types of Prosochit®, *Prosopis* gum (PRG), and chitosan (CTS) separately as emulsifiers for the outer emulsion. The formulations were analyzed for particle size, drug release, and permeation. Particle sizes of the Prosochit®-based formulations were found to be 10.40–13.85 nm (for the inner emulsion) and 128.00–160.40 nm (for the outer emulsion). Prosochit® limited the drug release at the gastric pH to a maximum of 10.1%. The maximum values of drug release in phosphate buffer pH 6.8 were 66.2%, 61.5%, 65.3%, 61.3%, and 58.2% while the permeation values were 49.8%, 53.8%, 49.1%, 54.9%, and 57.6% for the formulations containing PRG, Prosochit® 201, Prosochit® 101, Prosochit® 102, and CTS, respectively. The three types of Prosochit®-based nanoparticles have comparable controlled release and permeation properties and are superior to PRG -based and CTS -based nanoparticles for oral delivery of insulin.

INTRODUCTION

Poor adherence is a major problem with the parenteral administration of insulin because of the associated pain at the site of injection. Consequently, the oral route has emerged as a viable option for administering the drug. Oral insulin mimics the endogenous insulin route as it is directly delivered to the liver through the portal vein (Arbid and Kidron, 2017). However, it faces the challenges of degradation by proteolytic enzymes due to the chemical nature of the drug as well as poor intestinal absorption because of its molecular size (Zhang *et al*., 2008). It is therefore essential to address these two challenges before attempting the oral delivery of the drug.

**Corresponding Author*
Emmanuel O. Olorunsola, Department of Pharmaceutics and Pharmaceutical Technology, University of Uyo, Uyo, Nigeria.
E-mail: olorunsolaeo @ yahoo.com

Incorporation of enzyme inhibitors into oral formulations of insulin has been employed to mitigate the activity of proteolytic enzymes (Agarwal *et al*., 2001). In another approach to prevent the activity of proteolytic enzymes, insulin was encapsulated using Cholestosomes® (neutral, lipid-based particles), which is capable of passing through the gastrointestinal tract without being digested and releasing the insulin after absorption (McCourt *et al*., 2020). Furthermore, smart drug delivery systems have been employed for delivering medicaments such as proteins, vaccines, and anticancer agents to targeted locations in the body (Madkour, 2019; Mehanna *et al*., 2014).

Bile salts, surfactants, calcium ion-chelating agents, and fatty acids are some of the traditional absorption enhancers that have been used to promote the absorption of protein drugs, such as insulin (Mesiha *et al*., 1994). They either modulate the structure of the cellular membrane during transcellular absorption or alter the tight junctions between cells of the intestinal epithelium during paracellular absorption (Salama *et al*., 2006). However, one of the

drawbacks of using absorption enhancers is that some of them such as bile salts and nonionic surfactants have intrinsic toxicity (Salama *et al*., 2006; Swenson *et al*., 1994). On the contrary, chitosan, a natural linear biopolyaminosaccharide, has been shown to be a safe absorption enhancer (Kumar *et al*., 2004; Olorunsola *et al*., 2016; Zuorro *et al*., 2021).

Polymer nanoparticles are now widely used biomaterials for drug delivery because of their beneficial properties in terms of simplicity and biocompatibility (Madkour, 2019). Natural polymers such as *Prosopis* gum (PRG) and chitosan (CTS) have several advantages over synthetic ones because of their low cost, nontoxicity, biodegradability, and availability. While PRG has been used for controlled drug delivery and for inhibiting drug release at the gastric pH (Nadaf *et al*., 2015; Olorunsola *et al*., 2017), CTS has been used to enhance intestinal absorption (Kos *et al*., 2008).

Prosochit®, which is being used in this work to generate the nanoparticles of insulin, is a composite of PRG and crab shell CTS. Different types of Prosochit® have been synthesized using different proportions of the two components. Prosochit® 201 (PC201) is a composite of 66.67% PRG and 33.33% crab shell CTS, Prosochit® 101 (PC101) is a composite of equal proportions of the two polymers while Prosochit® 102 (PC102) is a composite of 33.33% PRG and 66.67% crab shell CTS. These excipients have been investigated for oral tablet formulation of hydrochlorothiazide, with PC201 used at 3% binder concentration producing the best result (Olorunsola *et al*., 2021).

This work aims at developing and characterizing Prosochit®-based nanoparticles of insulin for oral delivery. Different types of Prosochit® will be investigated since they have been found to have the same chemical composition but different physical properties due to the differences in the proportion of the component polymers (Olorunsola and Usungurua, 2018). The uniqueness of this work is the combined merits of (i) ability of PRG to inhibit drug release at the gastric pH; (ii) ability of the oil as the middle phase of the water-in-oil-in-water (w/o/w) emulsion to preserve insulin against proteolytic enzymes; (iii) utilization of nanotechnology for particle size reduction to enhance absorption; and (iv) ability of CTS to enhance intestinal absorption of insulin. These factors are potential mechanisms for addressing the drawbacks of the oral delivery of insulin.

MATERIALS AND METHODS

Materials

The materials used include PC201, PC101, and PC102 as well as PRG from *Prosopis africana* seeds and CTS from *Callinectes gladiator* shells, all prepared as described by Olorunsola (2017). Other materials used are soluble insulin powder from bovine pancreas (Lot No. SLB25307, Sigma-Aldrich Chemie GmbH, Germany), liquid paraffin, Span 60, sodium hydroxide (BDH Chemicals, England), and hydrochloric acid (Fisher Scientific International Company, USA).

Compatibility studies

Differential scanning thermograms of soluble insulin, a simple mixture of the three types of Prosochit®, and a simple mixture of PC101and soluble insulin were obtained. The analysis was carried out in an A1 40 ul crucible using a DSC-204F1 machine (NETZSCH Co., Germany), and the scanning was done at a 20°C/minute heating rate over a temperature range of 30°C–250°C.

The Fourier transform infrared (FTIR) spectra of the three samples (soluble insulin powder, mixture of the three types of Prosochit®, and insulin–PC101mixture) were obtained. Each sample was prepared on a potassium bromide disk, and the spectrum was recorded over a scanning range of 500–4,000/cm using a spectrophotometer (Model 8400S, Shimadzu Corporation, Kyoto, Japan).

Preparation of insulin-loaded Prosochit® nanoparticles

The w/o/w double emulsion method described by Mumuni *et al*. (2020) was employed with slight modification. Five batches of nanoemulsions containing different polymers as the emulsifier for the outer emulsion (as shown in Table 1) were prepared as w/o/w double emulsions. The polymers used as emulsifier for the outer emulsion of batches F1 to F5 were PRG, PC201, PC101, PC102, and CTS, respectively.

Span 60 (0.2 g) and liquid paraffin (20 ml) were placed in a 100 ml capacity beaker containing a magnet. The emulsifier and the oil were homogenized for 10 minutes using a magnetic

Table 1. Quantities of the various materials used for preparing each batch of nanoparticles.

Ingredients	F1	F2	F3	F4	F5
Soluble insulin (g)	0.18	0.18	0.18	0.18	0.18
Purified water (ml)	5.00	5.00	5.00	5.00	5.00
Span 60 (g)	0.20	0.20	0.20	0.20	0.20
Liquid paraffin (ml)	20.00	20.00	20.00	20.00	20.00
PRG	8.58	—	—	—	—
PC201	—	8.58	—	—	—
PC101	—	—	8.58	—	—
PC102	—	—	—	8.58	—
CTS	—	—	—	—	8.58
0.2 N HCl (ml)	49.60	49.60	49.60	49.60	49.60
0.1 N NaOH (ml)	99.20	99.20	99.20	99.20	99.20

stirrer with a hot plate at 1,000 rpm. In another beaker, 0.18 g (500 IU) soluble insulin was dissolved in 5 ml purified water. The solution of the soluble insulin was added slowly to the content of the first beaker, and the dispersion was homogenized at 1,000 rpm for 10 minutes.

To another beaker, 8.58 g of the emulsifier for the outer emulsion was placed, and 49.60 ml of 0.2 N HCl was added to disperse the emulsifier by homogenization at 1,000 rpm for a period of 10 minutes. This was followed by the addition of a sufficient amount of 0.1 N NaOH for neutralization. The initial emulsion containing insulin was gradually added with continuous homogenization at 1,000 rpm for another 10 minutes. The prepared nanoemulsions were freeze-dried for three days using a Clifton freeze-dryer to obtain the appropriate nanoparticles, and the final weight of each batch was determined.

Particle size analysis

A charged colloidal dispersion of nanoparticles was placed in a zeta cell. Upon the application of an external electric field, the particle sizes of the inner and outer emulsions were recorded using the Zetasizer (Nano ZS Malvern Panalytical).

Standard calibration curve of insulin

Several concentrations (0.25, 0.50, 1.00, 1.50, 2.00, and 2.5 µg/ml) of insulin in 0.01 M HCl were prepared as described by Najjar *et al*. (2014), and their absorbances were read at the wavelength of 271 nm using a UV spectrophotometer (L7 Double Beam UV-VIS Spectrophotometer, China). A graph of absorbance versus concentration was plotted to obtain the standard calibration curve of insulin, which was used in determining drug loading capacity, percent drug released, and percent drug permeated.

Determination of drug loading capacity

A 250 mg quantity of insulin-loaded nanoparticles was transferred into a 20 ml test tube containing 10 ml of 0.01 M HCl, and the test tube was shaken vigorously. The dispersion was centrifuged at 1,500 rpm for 5 minutes, after which the supernatant was collected. The supernatant was filtered and analyzed at 271 nm (L7 Double Beam UV-VIS Spectrophotometer, China). The amount of insulin loaded into the nanoparticles was determined by relating the absorbance to the standard calibration curve of insulin. The drug loading capacity of the nanoparticles was calculated using the following equation (Massella *et al*., 2018):

$$\text{drug loading capacity} = \frac{\text{amount of insulin in the nanoparticles}}{\text{amount of nanoparticles taken}} \times 100. \quad (1)$$

In vitro drug release studies

A modified form of the method described by Mumuni *et al*. (2020) was used for the drug release studies. Insulin-loaded nanoparticle quantities containing 1.75 mg drug were filled into hard gelatin capsules. Each capsule was placed in the dry basket of a United States Pharmacopoeia (USP) dissolution apparatus (Type RCZ-6C3, China) containing 500 ml dissolution medium pH 1.2 maintained at 37°C ± 0.5°C. The apparatus was set to a rotational speed of 100 rpm and allowed to operate for 2 hours. Aliquots (5 ml) were withdrawn at 20 minutes intervals with subsequent replacement with fresh dissolution medium. The procedure was repeated using phosphate buffer pH 6.8 as the dissolution medium and sampling was done at 30 minutes intervals for a period of 2 hours and then hourly for the following 6 hours. Each withdrawn sample was filtered through a Whatman filter paper No. 2 and assayed at the wavelength of 271 nm using the L7 Double Beam UV-VIS Spectrophotometer (China). The cumulative percent drug released was calculated using the following equation, and a graph of the cumulative percent drug released against time was plotted in both cases:

$$\text{Cum. \% drug released} = \frac{\text{concentration} \times \text{volume of medium used}}{\text{weight of drug used}} \times 100. \quad (2)$$

Ex vivo permeation studies

Drug permeation of the nanoparticles in a freshly prepared phosphate buffer solution pH 6.8 was studied using the jejunum of a freshly sacrificed pig as the permeation membrane. Insulin-loaded nanoparticles equivalent to 1.75 mg insulin each was weighed and transferred into a segment of the pig's jejunum already tied at one end and containing 5 ml of the phosphate buffer solution. The jejunum section containing the dispersed nanoparticles was tied at the other end to constitute the donor compartment.

The receiving medium (500 ml phosphate buffer solution pH 6.8 contained in USP dissolution apparatus Type RCZ-6C3) was heated to 37°C ± 0.5°C. Each donor compartment was placed in the receiving medium and tied to the dissolution apparatus set to a rotational speed of 100 rpm. Aliquots (5 ml) were withdrawn at 1 hours intervals over 8 hours with subsequent replacement using fresh dissolution medium maintained at the same temperature. Each withdrawn sample was filtered through a Whatman filter paper No. 2, and the filtrate was assayed at the wavelength of 271 nm. The cumulative percent drug permeated was calculated using Equation (2), and a graph of the cumulative percent drug permeated was plotted against time.

Statistical analysis

Statistical analysis was carried out using the GraphPad InStat software. The experimental data were analyzed by one-way ANOVA, which was followed by Tukey–Kramer multiple comparison test with the significance of difference taken as $p < 0.05$.

RESULTS AND DISCUSSIONS

Compatibility of Prosochit® with insulin based on differential scanning calorimetry

The differential scanning calorimetry (DSC) thermograms of the pure ingredients (insulin powder and Prosochit®) and the physical mixture of the two ingredients are shown in Figure 1. The curves indicated exothermic peaks upward and endothermic peaks downward. The thermogram of pure insulin was characterized by two endotherms comprising a wide endotherm with a peak at 65°C and a sharp endotherm with a peak at 95°C; that of Prosochit® showed a wide endotherm with a peak at 103°C while

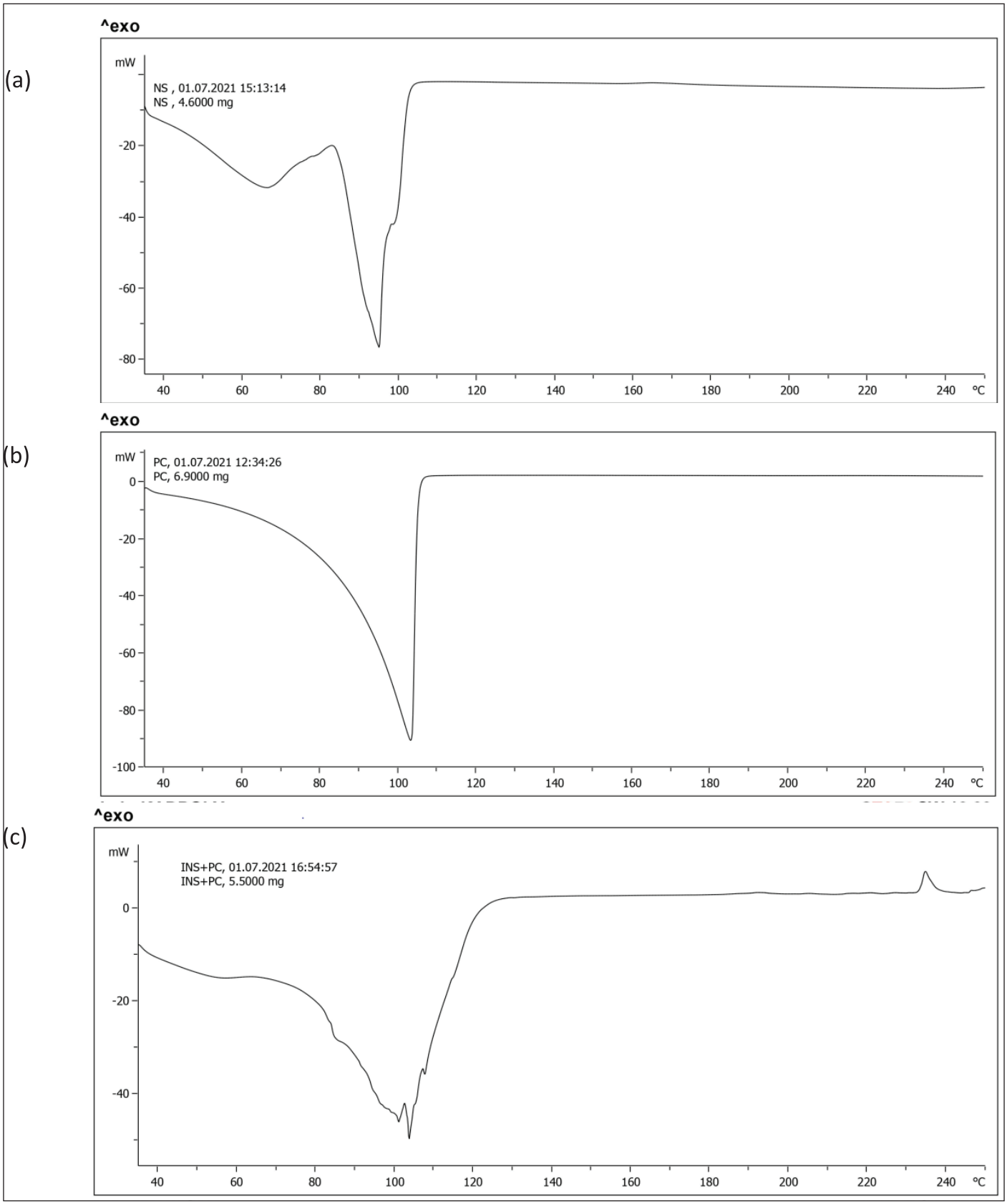

Figure 1. Differential scanning thermograms of (a) insulin, (b) Prosochit®, and (c) insulin + Prosochit®.

that of the insulin-Prosochit® mixture showed a wide endothermic transition and a normal exothermic transition.

The first endotherm of the thermogram of insulin can be ascribed to enthalpy relaxation while the second one can be ascribed to the melting of the drug (Fig. 1a). The long span of the enthalpy relaxation (35°C–83°C) is an indication of the presence of numerous segments of insulin, the 51 amino acids, while the peak of the second endotherm (95°C) reflects the melting point of the soluble insulin. This is similar to the melting point of 93.75°C reported for insulin by Jorge *et al*. (2020). The endotherm in the thermogram of Prosochit® (Fig. 1b) can be ascribed to the enthalpy relaxation of the polymer, and the width shows the polymeric nature of the substance (Miki *et al*., 2012).

The first peak at position 100°C within the endothermic transition in the thermogram of the mixture of insulin and Prosochit® can be ascribed to the enthalpy relaxation of insulin and that of Prosochit® that have been superimposed while the second peak at position 103°C can be ascribed to the melting of insulin. The presence of Prosochit® has increased the melting point of insulin to 103°C. The broad nature of the single endotherm in Figure 1c with no new peak being formed within the region is an indication that there was no observed adverse interaction between insulin and Prosochit®. The appearance of an exothermic transition with a peak at 235°C is an indication of polymer degradation (Olorunsola *et al*., 2016). Since such transition was not observed in the thermogram of the pure Prosochit®, it can be inferred that the presence of insulin hastened the degradation of Prosochit®.

Compatibility of Prosochit® with insulin based on FTIR spectroscopy

The FTIR spectra of insulin, Prosochit®, and the mixture of the two ingredients are shown in Figure 2. The FTIR spectrum of insulin showed many absorption peaks between 834.9 and 3,280.1 cm^{-1} while that of Prosochit® showed unique peaks between 693.3 and 3,697.5 cm^{-1} with strong signals between 693.3 and 1,401.1 cm^{-1}. All the major peaks observed in the FTIR spectrum of insulin (Fig. 2a) were retained in the spectrum of the insulin-Prosochit® mixture (Fig. 2c), the only difference being a slight shift in the position of some of the peaks.

The absorption peak at 834.9 cm^{-1} in the spectrum of insulin (Fig. 2a) is indicative of the C-H bending of the aromatic ring. The two absorption peaks at 1,129.4 and 1,174.1 cm^{-1} (1,000–1,200 cm^{-1}) are indicative of aliphatic C-N stretching while those between 1,340 and 1,480 cm^{-1} are indicative of C-H bending of CH_2. The absorption peak at 1,513.3 cm^{-1} reflects the stretching of the aromatic carbon–carbon double bond while that at 1,643.8 cm^{-1} shows the presence of amide since peaks occurring between 1,550 and 1,650 cm^{-1} indicate N-H bending and 1,630–1,690 cm^{-1} indicate C=O of amide. The absorption peak between 2,500 and 3,000 cm^{-1} indicates O-H of carboxylic acid while the peak at 3,280.1 cm^{-1} can be ascribed to the N-H stretching of amide (Coutts, 2008). All these features are typical of an insulin molecule (Lima *et al*., 2014).

The strong signals detected between 693.3 and 1,401.1 cm^{-1} in the spectrum of Prosochit® indicate C-H bending of the aromatic ring while the peaks at 1,483.5 and 1,636.3 cm^{-1} are indicative of the carbon–carbon double bond (Fig. 2b). The appearance of some peaks in the single-bond region (2,500–3,400 cm^{-1}) indicates the presence of an aromatic ring while those appearing beyond 3,600 cm^{-1} are reflective of nonbonded O-H, as explained by Coutts (2008). All these features are indicative of Prosochit® (Olorunsola *et al*., 2021).

FTIR spectroscopy is useful for characterizing unknown substances, detecting the decomposition of a substance, identifying the interaction between two substances, or detecting the presence of impurities (La Russa *et al*., 2009), but, in this study, it was used to investigate the potential interaction between insulin and Prosochit®. Since there is no major difference in the spectra of insulin and that of the insulin-Prosochit® mixture, it can be concluded that no adverse interaction was observed between insulin and Prosochit®.

Particle size and drug loading capacity

The results obtained from the particle size analysis and drug loading investigation of the nanoparticles of the various batches are summarized in Table 2.

There was a significant difference ($p < 0.0001$) in the particle size of the emulsion facilitated by PRG (F1) compared to that facilitated by CTS (F5), the one facilitated by PRG being smaller. The observation is true for both the inner and outer emulsions. The particle sizes of the emulsions facilitated by the three types of Prosochit® were not significantly different, and they are all on the nanoscale. An increase in CTS concentration and a decrease in PRG concentration led to an increase in the particle size of the nanoparticles.

The nanodimension and the insignificantly different particle sizes of the emulsions facilitated by the three types of Prosochit® (F2–F4) are indications that the three types of Prosochit® are suitable for the formulation of w/o/w nanoparticles of insulin. Of these three formulations, PC101 produced nanoparticles with the largest particle size of the inner emulsion and the smallest particle size of the outer emulsion; thus, it is the most efficient in formulating the nanoparticles. The oil phase in the nanoparticles stabilizes insulin against the activity of proteolytic enzymes. This is based on the explanation provided by McCourt *et al*. (2020) that the encapsulation of insulin in a lipid system protects it against proteolytic enzymes.

The particle size of an emulsion can be influenced by the quantity of polymer used as an emulsifier and the viscosity of the continuous phase. Hence, the difference in the particle sizes of the nanoparticles can be attributed to the different types and proportions of polymers used in formulating the nanoparticles. This explains the observed increase in particle size of the insulin nanoparticles with an increase in CTS concentration and with a decrease in PRG concentration.

The drug loading capacity of the nanoparticles ranged from 0.74% to 1.15%, with the mean value being 1.044%. The batch containing PRG was characterized by the highest drug loading capacity while that containing CTS was characterized by the lowest capacity. The expression "drug loading capacity" shows the ratio of the entrapped drug to the total weight of the carrier system or formulation. Hence, of the polymers investigated, PRG demonstrated the highest capacity for delivering insulin.

The values of deviation from the mean drug loading capacity showed that PRG and the three types of Prosochit® are significantly different from CTS. However, the eventual drug

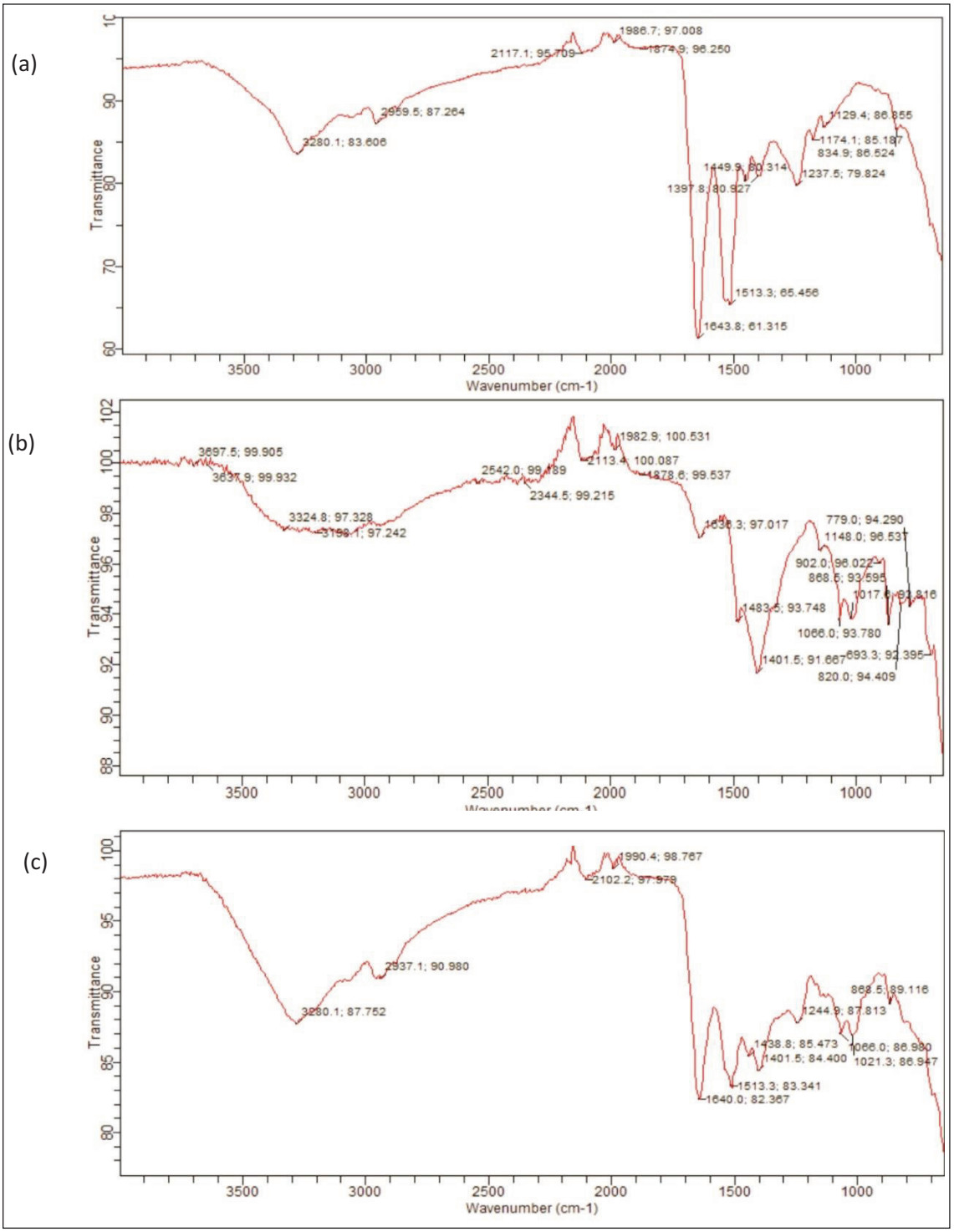

Figure 2. FTIR spectra of (a) insulin, (b) Prosochit®, and (c) insulin + Prosochit®.

loading of the nanoparticles can be modified by controlling the extent of drying. The main objective of the formulation is to protect and deliver the incorporated insulin to the site where absorption would take place.

In vitro drug release

Patterns of drug release from the formulated insulin-loaded nanoparticles in dissolution media pH 1.2 and 6.8 are illustrated in Figures 3 and 4, respectively.

For drug release in dissolution medium pH 1.2, there was an initial burst release to the extent of 9.1% to 12.0% within 20 minutes (0.33 hours), with the highest value being observed with CTS. Burst release has been found to be associated with protein-loaded nanoparticles, and this must be minimized as much as possible as proteins are not stable under the gastric condition (Jorge *et al*., 2020). After the burst release, drug dissolution up to time 2 hours did not change significantly, showing that the formulations were able to inhibit drug release at the gastric pH. It can also be inferred that the rate of drug degradation at the gastric

Table 2. Particle sizes and drug loading capacity of the various nanoparticles.

Batch	Particle size of the inner (water-in-oil) emulsion (nm)	Particle size of the outer (oil-in-water) emulsion (nm)	Drug loading capacity (%)	Deviation from mean loading capacity
F1	0.62 ± 0.00	328.9 ± 48.79	1.15	+ 0.11
F2	10.84 ± 1.70	151.3 ± 16.02	1.08	+ 0.04
F3	13.85 ± 4.27	128.0 ± 38.64	1.12	+ 0.08
F4	10.40 ± 2.20	160.4 ± 38.12	1.13	+ 0.09
F5	373.20 ± 92.89	5,441.0 ± 275.20	0.74	− 0.30

F1 = nanoparticles with PRG as emulsifier; F2 = nanoparticles with PC201 as emulsifier; F3 = nanoparticles with PC101 as emulsifier; F4 = nanoparticles with PC102 as emulsifier; F5 = nanoparticles with CTS as emulsifier.

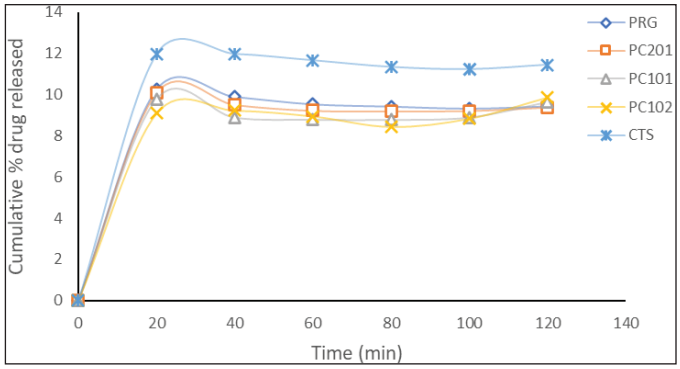

Figure 3. Release profile of insulin-loaded nanoparticles in dissolution medium pH 1.2 (PRG = nanoparticles of *Prosopis* gum; PC201 = nanoparticles of Prosochit® 201; PC101 = nanoparticles of Prosochit® 101; PC102 = nanoparticles of Prosochit® 102; CTS = nanoparticles of chitosan).

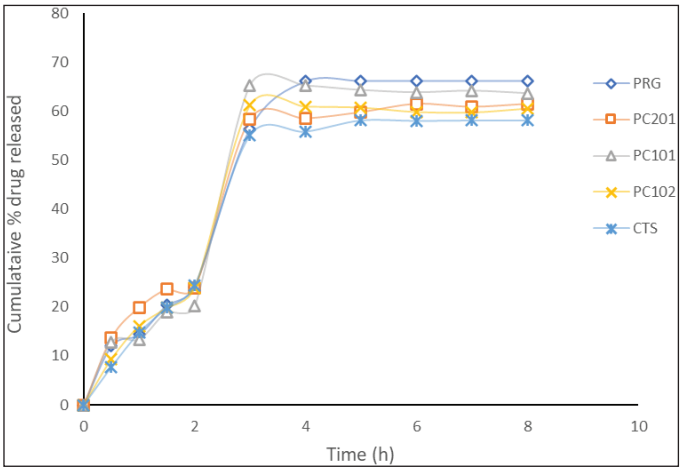

Figure 4. Release profile of insulin-loaded nanoparticles in phosphate buffer pH 6.8 (PRG = nanoparticles of *Prosopis* gum; PC201 = nanoparticles of Prosochit® 201; PC101 = nanoparticles of Prosochit® 101; PC102 = nanoparticles of Prosochit® 102; CTS = nanoparticles of chitosan).

pH is not significantly higher than the slow drug dissolution after the burst release.

At the gastric pH, the maximum drug release observed with formulations containing Prosochit® was 10.1%. The three types of Prosochit® and PRG are not significantly different and are superior to CTS in inhibiting the release of insulin at this pH. The highest drug release observed with CTS at the gastric pH can be explained by the fact that CTS is more soluble while PRG is more swellable at acidic pH (Olorunsola *et al.*, 2017).

Drug release in the phosphate buffer pH 6.8 was more, and it increased consistently up till time 3–4 hours after which it became constant for all the batches. Like the drug release at the gastric pH, the release in phosphate buffer pH 6.8 was characterized by an early burst effect. This was however followed by a further consistent release until the peaks were attained.

The earliest peak was obtained with PC101 at time 3 hours, an observation that can be attributed to the combined effect of PRG and CTS. However, the highest peak of 66% was observed with Formulation 1 (containing PRG) at time 4 hours. The delay in drug release by PRG is attributable to its high adhesive strength while its effectiveness in ensuring eventual drug release can be attributed to its increased solubility at higher pH (Olorunsola *et al.*, 2017).

In the presence of acid and proteolytic enzymes, peptide drugs such as insulin are degraded and their biological activity is reduced. The stomach has an acidic pH, and proteolytic enzymes are present across the gastrointestinal tract, but the ileum possesses the least activity (Whitcomb and Lowe, 2007). It is therefore very essential to design oral insulin to be protected from early drug release. The nanoparticles provided substantial protection for insulin against early drug release, thereby minimizing the effect of acid degradation and proteolysis.

Ex vivo drug permeation

Permeation profiles of all the formulated nanoparticles are illustrated in Figure 5, with the results of the studies presented for up to 8 hours. The maximum drug permeated values are 49.8%, 53.8%, 49.1%, 54.9%, and 57.6% for F1–F5 coded PRG, PC201, PC101, PC102, and CTS, respectively.

Chitosan is a permeation enhancer, hence the distinct permeation profiles of Formulation F5 (containing CTS) and Formulation F4 (which contains PC102 with a high proportion of CTS). *Prosopis* gum is a strong mucoadhesive agent, and this could explain why it performed slightly better than PC101, which produced the lowest percent permeation. Even though PC101 is a composite of PRG and CTS, the quantities of the two polymers are low, hence the poor permeation-enhancing effect. An excipient must be at the optimal concentration for it to perform optimally.

Absorption of insulin relies mainly on the paracellular route, which is restricted by tight junctions (Bourdet *et al.*, 2006). Therefore, the presence of CTS, a permeation enhancer that works by widening the tight junction, is necessary for promoting the absorption of oral insulin. CTS also improves protein stability and lengthens its duration of action in systemic circulation (Mohammed *et al.*, 2007). Hence, CTS is a necessary ingredient for an oral delivery system of insulin.

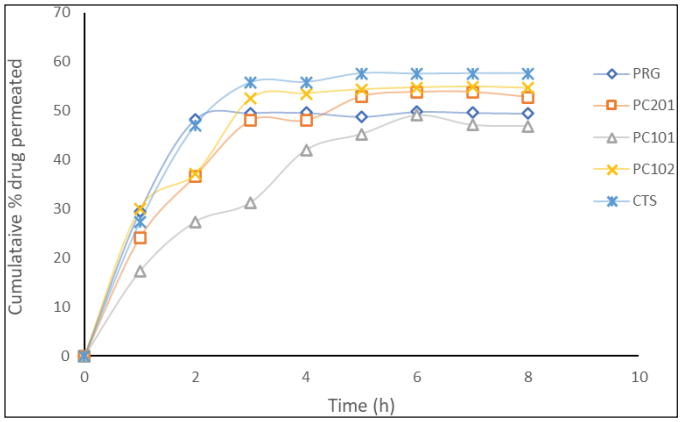

Figure 5. Permeation profiles of insulin-loaded nanoparticles (PRG = nanoparticles of *Prosopis* gum; PC201 = nanoparticles of Prosochit® 201; PC101 = nanoparticles of Prosochit® 101; PC102 = nanoparticles of Prosochit® 102; CTS = nanoparticles of chitosan).

CONCLUSION

Only minimal interaction occurs between Prosochit® and insulin, and the polymer can be used for the formulation of insulin without causing any obvious adverse effect. The findings suggest that Prosochit® serves as a means of combining the controlled release effect of PRG and the permeation-enhancing effect of CTS, with the different types of the novel excipient having different effects on drug release and permeation. PC101is characterized by the best-controlled release while PC102 and PC201are characterized by a better permeation-enhancing effect. This study has shown the potential of the three Prosochit®-based nanoparticulate systems for the oral delivery of insulin. Further work should be done as preclinical trials using animal models to advance the studies on this delivery system.

FINANCIAL SUPPORT

This work was supported by the Nigerian Tertiary Education Trust Fund through the 2019 National Research Grant (Reference No. TETFund/DR&D/CE/NRF/STI/37/VOL1).

AUTHORS' CONTRIBUTIONS

Emmanuel Olorunsola contributed to the conceptualization, project design, and drafting of the manuscript. Koofreh Davies contributed to data validation and critical revision of the manuscript. Koton Ibiang, Patience Etsuga, and Ezinne Uwaechi contributed to the acquisition of data and drafting of the manuscript. Fakhrul Ahsan contributed to the design of the work and critical revision of the manuscript for intellectual content. All the authors gave approval for the version sent for publication

CONFLICTS OF INTEREST

One of the used excipients (Prosochit®) is an innovation by one of the authors (Emmanuel Olorunsola).

ETHICAL APPROVAL

Approval for experimentation involving laboratory animals was obtained from the Animal Research Ethics Committee of the University of Uyo, Uyo, Nigeria (Protocol No. UU/Pharm/2019/14). The work was carried out based on the National Research Council's Guide for the Care and Use of Laboratory Animals.

DATA AVAILABILITY

All data generated and analyzed are included in this research article.

PUBLISHER'S NOTE

This journal remains neutral with regard to jurisdictional claims in published institutional affiliation.

REFERENCES

Agarwal V, Reddy IK, khan MA. Polymethyacrylate-based microparticulates of insulin for oral delivery: preparation and *in vitro* dissolution stability in the presence of enzyme inhibitors. Int J Pharm, 2001; 225(1–2):31–9.

Arbid E, Kidron M. Oral insulin delivery in a physiologic context: review. J Diab Sci Tech, 2017; 11(4):825–32.

Bourdet DL, Pollack GM, Thakker DR. Intestinal absorptive transport of the hydrophilic cation ranitidine: a kinetic modeling approach to elucidate the role of uptake and efflux transporters and paracellular vs. transcellular transport in Caco-2 cells. Pharm Res, 2006; 23:1178–87.

Coutts RT. Infrared spectroscopy. In: Chatten LG (ed.). Pharmaceutical chemistry - instrumental techniques, CBS Publishers and Distributors PVT Ltd, New Delhi, India, pp 59–125, 2008.

Jorge LR, Harada LK, Silva EC, Campos WF, Moreli FC, Shimamoto G, Pereira JFB, Oliveira Jr JM, Tubino M, Vila MMDC, Balcao VM. Non-invasive transdermal delivery of human insulin using ionic liquid: *in vitro* studies. Front Pharmacol, 2020; 11:243.

Kos MK, Boqataj M, Mrhar A. Heparin decreases permeability of pig urinary bladder wall preliminarily enhanced by chitosan. Drug Dev Ind Pharm, 2008; 34(2):215–20.

Kumar M, Muzzarelli R, Muzzarelli C, Sashiwa H, Domb A. Chitosan chemistry and pharmaceutical perspectives. Chem Rev, 2004; 104:6017–84.

La Russa MF, Ruffolo SA, Barone G, Crisci GM, Mazolleni P, Pezzino A, Francesco M. The use of FTIR and micro-FTIR spectroscopy: an example of application of cultural heritage. Int J Spectrosc, 2009; 893528:1–5.

Lima HA, Lia FMV, Ramdayal S. Preparation and characterization of chitosan-insulin-tripolyphosphate membrane for controlled drug release: effect of cross linking agent. J Biomater Nanobiotechnol, 2014; 50277:1–8.

Madkour LH. Nanoparticle and polymeric nanoparticle-based targeted drug delivery systems. In: Nucleic acids as gene anticancer drug delivery therapy, 2019; https://doi.org/10.1016/B978-0-12-819777-6.00013-5.

Massella D, Celasco E, Salaun F, Ferri A, Barresi AA. Overcoming the limits of flash nanoprecipitation: effective loading of hydrophilic drug into polymeric nanoparticles with controlled structure. Polymers, 2018; 10(10):1092.

McCourt M, Mielnicki L, Hughes J, Irving MQ, Schentag J, Ghanim H, Dandona P. 1013-P: modification of inflammatory and alzheimer markers with intracellular delivery of insulin using cholestosomes. Diabetes, 2020; 69(Suppl 1); https://doi.org/10.2337//db20-1013-P.

Mehanna MM, Mohyeldin SM, Elgindy NA. Respirable nanocarriers as a promising strategy for antitubercular drug delivery. J Contr Rel, 2014; 187:183–97.

Mesiha M, Plakogiannis F, Vejosoth S. Enhanced oral absorption of insulin from desolvated fatty acid-sodium glycocholate emulsions. Int J Pharm, 1994; 111:213–16.

Miki T, Sugimoto H, Kojiro K, Furuta Y, Kanayama K. Enthalpy relaxation behaviour with dry wood detected temperature-modulated DSC. J Wood Sci, 2012; 58:391–8.

Mohammed MA, Syeda JTM, Wasan KM, Wasan EK. An overview of chitosan nanoparticles and its application in non-parenteral drug delivery. Pharmaceutics, 2017; 20(9):53.

Mumuni MA, Ernest O, Ebele O, Kenechukwu F, Salome C, Chinekwu S, Aminu N, Ben A. Development and characterization of mucinated chitosan microcomposite for oral insulin delivery. Trop J Nat Prod Res, 2020; 4(11):1000–6.

Nadaf S, Nnamani P, Jadhav N. Evaluation of *Prosopis africana* seed gum as an extended-release polymer for tablet formulation. AAPS PharmSciTech, 2015; 16(3):716–29.

Najjar A, Alawi M, AbuHeshmeh N, Sallam A. A rapid, isocratic HPLC method for determination of insulin and its degradation product. Adv Pharm, 2014; 749823:1–6.

Olorunsola EO. Prosochit; a group of multifunctional pharma excipients. Nigerian Patent Registry, Abuja, Nigeria, NG/P/2016/00355; 2017.

Olorunsola EO, Adedokun MO, Bhatia PG, Tytler BA, Adikwu MU. Optimization of artesunate delivery by formulation in a delayed release prosopis hemicellulose matrix. J Appl Pharm Sci, 2017; 7(5):142–6.

Olorunsola EO, Adedokun MO, Samuel OU, Joseph MG. Effects of Prosochit® binder on the dissolution and permeation of a BCS class IV Drug. Trop J Nat Prod Res, 2021; 5(6):1138–41.

Olorunsola EO, Usungurua SG. Effect of polymer ratio on the quality of co-processed excipient of *Prosopis* gum and crab shell chitosan. Trop J Pharm Res, 2018; 17(9):1693–9.

Olorunsola EO, Uwah TO, Olayemi OJ, Etukudo UB. Ex-vivo evaluation of crab shell chitosan as absorption enhancer in ciprofloxacin tablet formulation. Afr J Biotehnol, 2016; 15(36):1930–35.

Salama NN, Eddington ND, Fasano A. Tight junction modulation and its relationship to drug delivery. Adv Drug Deliv Rev, 2006; 58(1):15–28.

Swenson ES, Milisen WB, Curatolo W. Intestinal permeability enhancement: efficacy, acute local toxicity and reversibility. Pharm Res, 1994; 11:1132–42.

Whitcomb D, Lowe M. Human pancreatic digestive enzymes. Dig Dis Sci, 2007; 52:1–17.

Zhang L, Jiang H, Zhu W, Wu L, Song L, Wu Q, Ren Y. Improving the stability of insulin in solutions containing intestinal proteases in vitro. Int J Mol Sci, 2008; 9(12):2376–87.

Zuorro A, Moreno-Sader KA, Gonzalez-Delgado AD. Inherent safety analysis and sustainability evaluation of chitosan production from shrimp exoskeleton in Colombia. Water, 2021; 13:553.

How to cite this article:
Olorunsola EO, Davies KG, Ibiang KP, Esukpa PC, Uwaechi EG, Ahsan F. Prosochit®-based nanoparticulate system of insulin for oral delivery: design, formulation and characterization. J Appl Pharm Sci, 2023; 13(03):044–052.